Protein *O*-mannosyltransferases participate in ER protein quality control

Veit Goder* and Alejandro Melero

Department of Genetics, University of Seville, Ave Reina Mercedes 6, 41012 Seville, Spain

*Author for correspondence (vgoder@us.es)

Accepted 9 November 2010
Journal of Cell Science 124, 144-153

doi:10.1242/jcs.072181

Summary

In eukaryotic cells, proteins enter the secretory pathway at the endoplasmic reticulum (ER) as linear polypeptides and fold after translocation across or insertion into the membrane. If correct folding fails, many proteins are *O*-mannosylated inside the ER by an *O*-mannosyltransferase, the Pmt1p–Pmt2p complex. The consequences of this modification are controversial and the cellular role of the Pmt1p–Pmt2p complex in this respect is unclear. Here, we have identified the binding partners of yeast Pmt1p and Pmt2p. These include ER chaperones involved in oxidative protein folding; the Hrd1p complex, which is involved in ER-associated protein degradation (ERAD); and the p24 protein complex involved in ER export. The results suggest that the Pmt1p–Pmt2p complex participates in these processes. We tested this assumption in a functional assay and found that whereas the Pmt1p–Pmt2p complex promotes fast ER export of the GPI-anchored protein Gas1p, it retains the misfolded version Gas1*p and targets it to the Hrd1p complex for subsequent degradation. Our results reveal previously unknown cellular roles of the Pmt1p–Pmt2p complex in connection with the ERAD machinery and show its participation in ER protein quality control.

Key words: Endoplasmic reticulum, ER protein quality control, ER-associated protein degradation, Pmt complex

Introduction

After translocation across or insertion into the endoplasmic reticulum (ER), membrane proteins have to fold, a process that is assisted by a variety of ER resident chaperones (for a review see Ellgaard and Helenius, 2003). Folding is monitored by ER quality control mechanisms, and correctly folded proteins are allowed to exit the ER by vesicular budding (Barlowe, 2003). Assistance in protein folding and quality control are often overlapping functions of ER chaperones. A folding intermediate is recognized by a chaperone through such universal signatures as exposed hydrophobic patches, unpaired cysteines, and proneness for aggregation (Fra et al., 1993; Hellman et al., 1999; Zhang et al., 1997). If initial folding is slow or fails, these features will continue to be exposed and will ensure immediate re-binding to a chaperone. By this mechanism, slow-folding proteins or proteins that misfold will be retained inside the ER for extended periods of time. Some ER retention mechanisms have additional complexity, such as the calnexin–calreticulin cycle found in mammalian cells, where several chaperones and enzymes together monitor the folding of glycoproteins (Hammond et al., 1994; Parodi, 2000).

As well as aiding in protein folding and ER retention, some universal chaperones such as calnexin and BiP possess a third function in that they can target terminally misfolded proteins for degradation (Brodsky et al., 1999; Denic et al., 2006; McCracken and Brodsky, 1996; Plemper et al., 1997). Degradation of aberrant ER proteins occurs mostly by a process called ER-associated protein degradation (ERAD), whereby proteins are 'retrotranslocated' into the cytosol to be degraded by the ubiquitin–proteasome system (for a review see Meusser et al., 2005). Core components of the responsible machineries for retrotranslocation are the ER membrane-embedded E3 ubiquitin ligases. In yeast, there are two such ubiquitin ligases, Doa10p and Hrd1p, which are found in distinct membrane protein complexes (Carvalho et al., 2006; Denic et al., 2006; Swanson et al., 2001). Together they promote retrotranslocation and degradation of most, if not all, misfolded substrates in the ER. Whereas the Doa10p complex targets membrane proteins with lesions in their cytosolic portions to the proteasome, a route termed the ERAD-C pathway, the Hrd1p complex retrotranslocates membrane proteins with misfolded transmembrane domains (ERAD-M pathway) or membrane and soluble proteins with defects in their luminal portion (ERAD-L pathway) (Carvalho et al., 2006; Vashist et al., 2001). All pathways converge at the cytosolic Cdc48p ATPase complex, which probably provides the energy for retrotranslocation and for substrate transfer to the proteasome (Carvalho et al., 2006; Rabinovich et al., 2002; Ye et al., 2001).

Whereas the vast majority of misfolded proteins of the secretory pathway are recognized early while still inside the ER and will ultimately be targeted for ERAD, there are cases where a fraction of these species exits the ER normally. This occurs if defective proteins are expressed in large quantities or if export signals are dominant enough that they compete with retention mechanisms (Caldwell et al., 2001; Haynes et al., 2002; Kincaid and Cooper, 2007; Vashist et al., 2001). In either case, it becomes more evident that the cell possesses additional, albeit less well-characterized, quality control mechanisms in post-ER compartments that can target aberrant proteins for degradation (Hettema et al., 2004; Hong et al., 1996; Reggiori and Pelham, 2002; Wang and Ng, 2010).

One interesting but poorly understood protein modification that occurs inside the ER is that of protein *O*-mannosylation, which is one of a variety of possible *O*-glycosylation events that occur throughout the secretory pathway (for a review see Spiro, 2002). *O*-mannosylation is mediated by members of the protein *O*-mannosyltransferase (PMT) family (Lussier et al., 1995; Strahl-Bolsinger et al., 1993). PMTs are multispanning membrane proteins

with seven transmembrane domains and two large luminal loops, which together are needed for the enzymatic activity (Girrbach et al., 2000; Strahl-Bolsinger and Scheinost, 1999). They are conserved from yeast to humans although they appear to be missing in plants (Willer et al., 2003). Single mannose residues are attached to side chains of one or several serine or threonine residues. It was reported that many proteins will be *O*-mannosylated inside the ER only in cases where they misfold (Harty et al., 2001; Vashist et al., 2001). The fate of misfolded proteins that have been *O*-mannosylated is controversial. Whereas some of them seem increasingly protected from degradation, others are reported to be degraded by the cytosolic proteasome to which they are targeted by an unknown mechanism (Harty et al., 2001; Hirayama et al., 2008). Interestingly, like most ER chaperones or members of the ERAD machineries, PMTs are upregulated during ER stress by the unfolded protein response (UPR) (Travers et al., 2000).

This study aimed at identifying the cellular role of the PMTs with respect to misfolded proteins. We identified the cellular binding partners of yeast Pmt1p and Pmt2p, which are known to form an active stochiometric complex (Pmt1p–Pmt2p) (Girrbach and Strahl, 2003). Binding partners include ER chaperones involved in oxidative protein folding; the Hrd1p complex, which is involved in ERAD; and the p24 protein complex, which is involved in protein ER export (Muniz et al., 2000; Schimmoller et al., 1995). These findings suggest that the Pmt1p–Pmt2p complex might participate in all these cellular processes. In a subsequent functional assay, we tested this hypothesis and showed that the Pmt1p–Pmt2p complex is required for fast ER export of the GPI-anchored protein Gas1p, whereas it retains the misfolded version Gas1*p and targets it to the Hrd1p complex for subsequent degradation. Our results put the Pmt1p–Pmt2p complex in a category with ER chaperones that function in ER protein quality control. We provide a model for how the machineries for protein *O*-mannosylation, ER export and ERAD are connected on a molecular level. Finally, our results unify previously contradicting data for the role of the Pmt1p–Pmt2p complex in ERAD.

Results

Interaction partners of Pmt1p and Pmt2p

To reveal the cellular function of the Pmt1p–Pmt2p complex, we first asked which components it is associated with. We separately tagged Pmt1p and Pmt2p chromosomally with a fusion tag that contained a Protein A moiety and a calmodulin binding peptide (CA tag) and expressed the proteins from their endogenous promoters. These tagged proteins were fully functional (supplementary material Fig. S1). Yeast cells were grown in volumes of 3 l. After cell lysis, membrane fractions were isolated and solubilized with 1% digitonin. Tagged proteins were affinity purified together with their binding partners using IgG-coupled magnetic beads. The eluate was subjected to SDS-PAGE followed by Coomassie Blue staining (Fig. 1A). The visualized bands were cut out and their identity determined by tandem mass spectrometry (Table 1 and supplementary material Table S1). Alternatively, we precipitated the entire eluate with trichloroacetic acid (TCA) and identified the pool of bound proteins by tandem mass spectrometry (Table 1 and supplementary material Table S1). A wild-type strain without tagged proteins was used as a control in all experiments.

As shown in Fig. 1A, Pmt1p and Pmt2p were isolated together but no abundant additional binding partners were visible (Fig. 1A, lanes 2 and 3, bands 1 and 2; Table 1). However, a faint smear was seen containing proteins of the p24 protein complex (Fig. 1A,

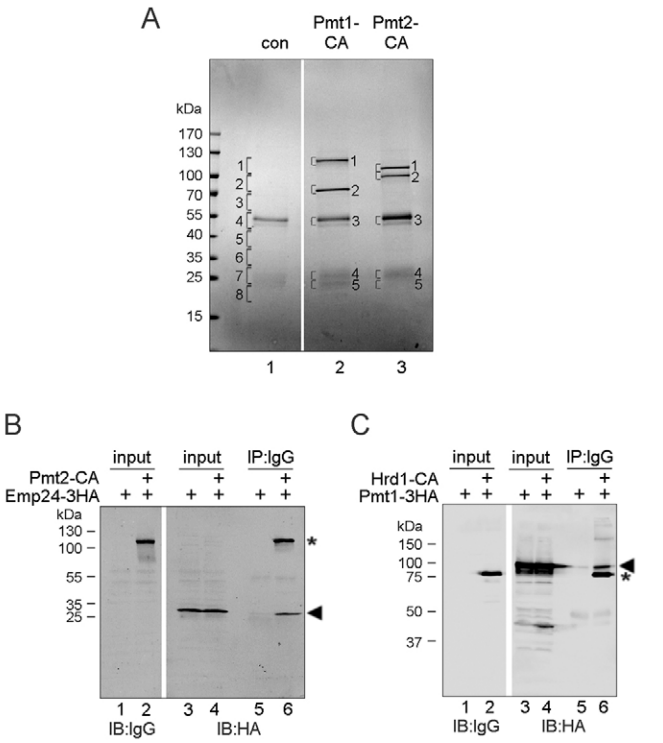

Fig. 1. The Pmt1p–Pmt2p complex associates with ER machineries involved in ER protein export and in ERAD. (**A**) Interaction partners of Pmt1p and Pmt2p. Wild-type yeast cells (con) or cells expressing either Pmt1-CA or Pmt2-CA were lysed and membrane fractions solubilized with 1% digitonin. The extract was incubated with IgG-coupled magnetic beads and bound material analyzed by SDS-PAGE and Coomassie Blue staining. Visualized bands (lanes 2 and 3) and regions from the control reaction (lane 1) were numbered, cut out and their protein content determined by mass spectrometry (Table 1; supplementary material Table S1). (**B**) Yeast cells expressing Emp24-3H with or without expressing Pmt2-CA were lysed. Samples were analyzed directly (input; 5% of total material) or after immunoprecipitation using IgG-coupled magnetic beads (IP:IgG; 95% of total material). All samples were separated by SDS-PAGE (4-20% gradient gel) and analyzed by immunoblotting (IB) with the indicated antibodies. The arrowhead indicates the co-immunoprecipitated fraction. The star indicates Pmt2-CA that was also recognized by the secondary antibody. (**C**) As for B, but using cells expressing Pmt1-3HA with or without expressing Hrd1-CA. The SDS-PAGE was performed using a 7% standard gel. The arrowhead indicates the co-immunoprecipitated fraction. The star indicates Hrd1-CA that was also recognized by the secondary antibody.

lanes 2 and 3, band 5; Table 1). In Fig. 1A, bands 3 and 4 contained residual IgG heavy and light chain from incomplete coupling to magnetic beads. Using TCA precipitation, we identified additional and less abundant binding partners of the Pmt1p–Pmt2p complex. Along with proteins of the p24 protein complex, we found Cdc48p, Hrd1p, Usa1p and Yos9p (components of the ERAD-mediating Hrd1p complex), Ero1p and Pdi1p (proteins involved in oxidative protein folding), Ubr1p and Cue4p (proteins involved in protein ubiquitylation), Dfm1p (a distinct co-factor of the Cdc48p ATPase) and Ted1p (a protein linked to GPI-anchor remodeling) (see Table 1).

In summary, the Pmt1p–Pmt2p complex associates weakly and thus probably transiently, with ER components that have established roles in protein folding and ER export as well as in ERAD. We

Table 1. Summary of interacting proteins that were immunoprecipitated with CA-tagged Pmt1p (Pmt1-CA) or CA-tagged Pmt2p (Pmt2-CA)

Interacting protein	Functional category	Tagged protein (bait)			
		Pmt1-CA		Pmt2-CA	
		Individual	Total	Individual	Total
Pmt1p	*O*-mannosylation	33[1]	36/32	35[2]	39/34
Pmt2p	*O*-mannosylation	28[2]	25/22	20[1]	22/21
Cdc48p	ERAD	–	1/2	–	18/3
Ero1p	Protein folding	–	2/2	–	3/2
Pdi1p	Protein folding	–	2/1	–	–/1
Hrd1p	ERAD	–	1/–	–	2/–
Usa1p	ERAD	–	2/–	–	2/2
Yos9p	ERAD	–	–/–	–	1/–
Ubr1p	Ubiquitin ligase	–	–/5	–	–/–
Dfm1p	Cdc48p cofactor	–	–/–	–	5/2
Cue4p	Ubiquitin binding	–	–/2	–	1/3
Ted1p	GPI remodeling	–	–/3	–	–/2
IgG hc		[3]		[3]	
IgG lc		[4]		[4]	
Emp24p	ER export (p24 complex)	–	2/2	–	2/2
Erv25p	ER export (p24 complex)	1[5]	6/4	–	5/4
Erp1p	ER export (p24 complex)	1[5]	5/5	2[5]	4/3
Erp2p	ER export (p24 complex)	–	2/2	4[5]	1/1

Bound proteins were identified using mass spectrometry. We analyzed either individual protein bands after their separation using SDS-PAGE and staining with Coomassie Blue (individual) or the total protein eluate after precipitation with trichloroacetic acid (total). Numbers indicate the number of peptides identified by mass spectrometry. For multiple experiments, numbers are separated by a solidus. The numbers in square brackets correspond to the bands in Fig. 1A. See supplementary material Table S1 for the complete set of mass spectrometry data. Although Yos9p was only identified with one individual peptide and would not pass our criteria as a true hit, we show it because it is a well-known Hrd1p complex component. IgG hc, immunoglobulin heavy chain; IgG lc, immunoglobulin light chain.

thus hypothesized that the Pmt1p–Pmt2p complex itself actively participates in these cellular processes.

Before testing our hypothesis experimentally we wanted to confirm and visualize the interactions of the Pmt1p–Pmt2p complex with the predominant binding partners that we identified: the Hrd1p complex and the p24 protein complex. To this end, we constructed strains in which two proteins were differentially tagged. As can be seen in Fig. 1B, a fraction of HA-tagged Emp24p (Emp24-3HA, a member of the p24 protein complex) co-precipitates with CA-tagged Pmt2p (Pmt2-CA). A control strain without Pmt2-CA did not bring down tagged Emp24p (Fig. 1B, compare lanes 5 and 6). As can be seen in Fig. 1C, we could co-isolate a fraction of HA-tagged Pmt1p (Pmt1-3HA) with CA-tagged Hrd1p (Hrd1-CA, the E3-ligase of the Hrd1p complex). Only faint background staining was visible if Hrd1p was untagged (Fig. 1C, compare lanes 5 and 6).

To assess whether degradation of the tagged Pmt1p–Pmt2p complex by the Hrd1p complex leads to their observed association, we performed a cycloheximide (CHX)-chase analysis of CA-tagged Pmt2p. Surprisingly, Pmt2-CA was relatively unstable and was degraded with an approximate half life of 1.5 hours (supplementary material Fig. S2). However, the turnover was independent of Hrd1p and thus the physical interaction was not due to degradation by the Hrd1p complex (supplementary material Fig. S2).

Gas1*p is a substrate for the Pmt1p–Pmt2p complex and is largely degraded by the ERAD-L pathway

To address our hypothesis that the Pmt1p–Pmt2p complex participates in protein folding, ER export and ERAD, we next looked for a suitable model substrate. Ideally, such a substrate should normally be exported from the ER in a p24 protein complex-dependent manner, whereas a mutant should be degraded via Hrd1p complex-mediated ERAD. The GPI-anchored protein Gas1p comes closest to these criteria. In its wild-type form, the protein leaves the ER depending on the p24 protein complex and is targeted to the plasma membrane (Muniz et al., 2001; Muniz et al., 2000; Schimmoller et al., 1995). Importantly, a mutant version of Gas1p, Gas1*p, is unstable and degraded by an unidentified proteasome-dependent pathway (Fujita et al., 2006). Interestingly, whereas Gas1p is *O*-glycosylated by Pmt4p and Pmt6p alone, Gas1*p is further *O*-glycosylated by Pmt1p and Pmt2p (Hirayama et al., 2008). Thus, the wild-type protein Gas1p and its mutant version Gas1*p appear well suited for our analysis.

We first confirmed that Gas1*p is *O*-mannosylated by the Pmt1p–Pmt2p complex as reported previously (Hirayama et al., 2008). To this end, we expressed chromosomally HA-tagged species of wild-type Gas1p [Gas1p(HA)] or mutant Gas1*p [Gas1*p(HA)] from their endogenous promoters in wild-type or in Pmt1–Pmt2 deletion mutant (Δpmt1Δpmt2) cells. We generally observed a lower protein expression level in Δpmt1Δpmt2 cells than in wild-type cells, which was also reflected in a reduced growth rate (data not shown). As can be seen in Fig. 2A, Gas1*p showed an increase in electrophoretic mobility in Δpmt1Δpmt2 cells as compared with wild-type cells, consistent with it being *O*-mannosylated (Fig. 2A, compare lanes 3 and 4, arrows). We occasionally observed a smear above the major protein bands, but because the phenomenon was rare we considered it unspecific. In contrast to Gas1*p, both the precursor and the mature form of Gas1p migrated with similar electrophoretic mobility in Δpmt1Δpmt2 and in wild-type cells (Fig. 2A, compare lanes 1 and 2). To exclude the possibility that the increase in electrophoretic mobility of Gas1*p in Δpmt1Δpmt2 cells results from defective *N*-glycosylation rather than from lack of *O*-mannosylation, we performed an additional set of experiments using the de-*N*-glycanase PNGase F to remove N-linked glycans prior to SDS-PAGE (supplementary material Fig. S3) and co-immunoprecipitation with the mannose-specific lectin Concanavaline A (supplementary material Fig. S4B). Finally, the

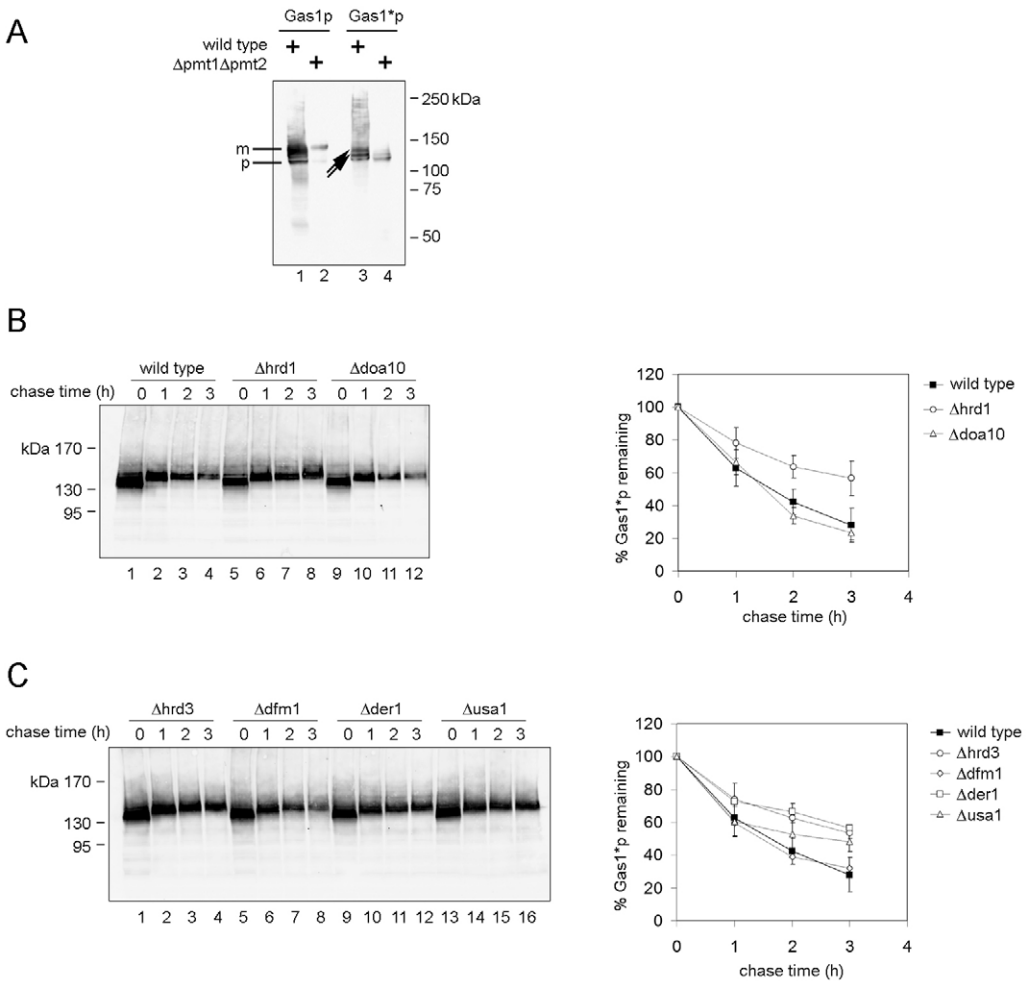

Fig. 2. The misfolded model protein Gas1*p is a substrate for the Pmt1p–Pmt2p complex and is in part degraded by the ERAD-L pathway. (**A**) Gas1p(HA) or Gas1*p(HA) were individually expressed in wild-type or in Δpmt1Δpmt2 cells. Equal amounts of cells were lysed and the proteins analyzed by SDA-PAGE (5% standard gel) followed by anti-HA immunoblotting. Arrows indicate the *O*-mannosylated fraction of Gas1*p: p, precursor form; m mature form. (**B**,**C**) The degradation of Gas1*p(HA) was measured in wild-type cells or in cells carrying the designated deletions after inhibition of protein synthesis by addition of 200 µg/ml cycloheximide. At the indicated time points, equal aliquots of cells were removed, lysed and the amount of remaining Gas1*p(HA) was analyzed by SDS-PAGE (4–20% gradient gel) followed by anti-HA immunoblotting. The bands were quantified by densitometry and the results of at least three independent sets of experiments were plotted (right panels).

aforementioned experiment to test for the functionality of tagged Pmt2p showed a Pmt2p-dependent change in electrophoretic mobility of Gas1*p over time (supplementary material Fig. S1). Together, these data confirm that Gas1*p but not Gas1p is modified in a Pmt1p–Pmt2p complex-dependent manner, strongly suggesting that Gas1*p interacts directly with the Pmt1p–Pmt2p complex and is *O*-mannosylated.

Next, we asked whether Gas1*p is degraded via the Hrd1p complex-dependent ERAD-L pathway as predicted on the basis of the fact that the misfolded GPI-anchored protein is exposed entirely to the lumen of the ER. To this end, we expressed Gas1*p in wild-type and deletion mutants of the Hrd1p complex and performed a CHX-chase experiment. As can be seen in Fig. 2B, lanes 1–4 and graph, when expressed in wild-type cells Gas1*p is degraded with a half-life of roughly 1.5 hours, consistent with previous data (Fujita et al., 2006). When we tested deletion mutants of all membrane-bound Hrd1p complex components (Hrd1p, Hrd3p, Der1p,and Usa1p), we found that they stabilized Gas1*p whereas deletion of Doa10p (the central component of the ERAD-C pathway) did not (Fig. 2B,C). Deletions of Dfm1p, Ubr1p or Cue4p (other binding partners of the Pmt1p–Pmt2p complex; Table 1) did not influence Gas1*p turnover (Fig. 2C and data not shown). These results show that Gas1*p is indeed targeted for degradation by the ERAD-L pathway. Our results are different from those published previously reporting that deleting Hrd1p had no effect on Gas1*p turnover (Fujita et al., 2006).

It has been reported that the p24 protein complex has a role in degradation of Gas1*p (Fujita et al., 2006). Because the p24 protein complex has an established function in ER export of wild-type Gas1p, the simplest scenario would be consistent with a p24 protein complex-dependent ER exit of a fraction of Gas1*p and its targeting for degradation from a post-ER compartment. However, our earlier results showed that both the Hrd1p complex and the p24 protein complex are present as associates of the Pmt1p–Pmt2p complex. It could thus be that the p24 protein complex interacts directly with the Hrd1p complex and has a role in targeting of Gas1*p to the

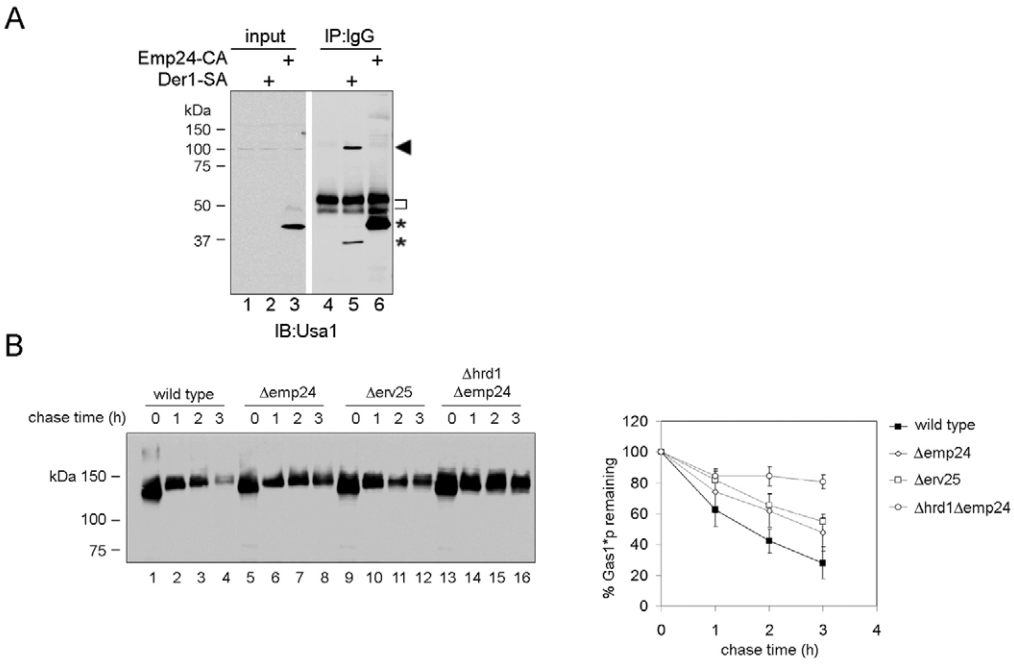

Fig. 3. The p24 protein complex does not interact with the Hrd1p complex and is part of an ERAD-L independent degradation pathway for a fraction of Gas1*p. (**A**) Wild-type cells (lanes 1 and 4) or cells expressing a tagged version of Der1p (Der1-CA; lanes 2 and 5) or Emp24-CA (lanes 3 and 6) were lysed and samples were analyzed as for Fig. 1B except that membranes were immunostained with anti-Usa1p antibodies. The SDS-PAGE was performed using a 7% standard gel. The arrowhead indicates co-immunoprecipitated fraction (note that the signal for Usa1p in the input fractions is low; lanes 1–3). Stars indicate Emp24-CA and Der1-CA that were also recognized by the secondary antibody. The bracket indicates IgG heavy chains that were recognized by the secondary antibody. (**B**) The degradation of Gas1*p(HA) was measured, quantified and plotted in wild-type cells or in cells carrying the designated deletions as described in Fig. 2. The SDS-PAGE was performed using a 7% standard gel.

ERAD machinery. To check this idea, we tested whether we could co-immunoprecipitate members of the ERAD machinery directly with Emp24p. As can be seen in Fig. 3A, we could not co-precipitate Usa1p (a member of the Hrd1p complex) with Emp24-CA, whereas the control reaction using CA-tagged Der1p (Der1-CA), another member of the Hrd1p complex, readily brought down Usa1p (Fig. 3A, compare lanes 4–6). Furthermore, we did not find Hrd1p complex components as binding partners of Emp24-CA when performing a large-scale pull-down experiment followed by mass spectrometric analysis, as described in Fig. 1 (V.G. and A.M., unpublished data). We then directly measured the degradation of Gas1*p in p24 protein complex deletion mutants. Deletions of either Emp24p or of Erv25p led to stabilization of Gas1*p (Fig. 3B, lanes 1–12), consistent with previous data (Fujita et al., 2006). This fraction was not secreted or targeted to the vacuole (V.G. and A.M., unpublished data). When we additionally disabled the ERAD-L pathway using Δhrd1Δemp24 deletion mutant cells we found maximal stabilization of Gas1*p (Fig. 3B, lanes 13–16 and graph). Together, these data suggest that Gas1*p can be degraded by two separate pathways: one is the ERAD-L pathway, which depends on the Hrd1p complex, and the other depends on the p24 protein complex and is consistent with leading to protein degradation from a post-ER compartment.

The Pmt1p–Pmt2p complex retains Gas1*p and ultimately targets it to the Hrd1p complex for degradation

Next, we directly addressed the role of the Pmt1p–Pmt2p complex in degradation of Gas1*p. The physical interaction of the Pmt1p–Pmt2p complex with the Hrd1p complex suggests that the Pmt1p–Pmt2p complex might target Gas1*p to the Hrd1p complex. In that case, absence of the Pmt1p–Pmt2p complex would lead to a stabilization of Gas1*p. If, alternatively, the Pmt1p–Pmt2p complex retains Gas1*p and prevents its retrotranslocation by the Hrd1p complex, its absence should result in faster degradation of Gas1*p. To distinguish between these possibilities, we performed a CHX-chase experiment with deletion mutants for either Pmt1p or Pmt2p or both. As can be seen in Fig. 4, deletion of the Pmt1p–Pmt2p complex drastically increases the turnover rate of Gas1*p, best visible for the Δpmt1Δpmt2 cells, in which the half life was reduced to approximately 45 minutes. This indicates that the Pmt1p–Pmt2p complex has an inhibitory function for the degradation of Gas1*p, consistent with an ER retention function for the misfolded protein.

As mentioned earlier, some classical ER chaperones such as BiP and calnexin are known to have multiple functions and play a role in protein folding, protein ER retention and in targeting for protein degradation. A similar function of the Pmt1p–Pmt2p complex to target substrates to the ERAD machinery or to the p24 protein complex could be masked by the retention effect that we observed. We thus constructed triple mutants in which we deleted Hrd1p or Emp24p in a Δpmt1Δpmt2 background and measured the degree of stabilization of Gas1*p. This allowed us to compare the amount of Gas1*p degraded by either pathway in the presence and absence of the Pmt1p–Pmt2p complex. As can be seen in Fig. 4B, both triple mutants stabilized Gas1*p as compared with Δpmt1Δpmt2 cells. However, the relative amount of Gas1*p degraded via the ERAD-L pathway was markedly reduced in the absence of the Pmt1p–Pmt2p complex, whereas most of the Gas1*p was degraded via a p24 complex-dependent pathway (Fig.

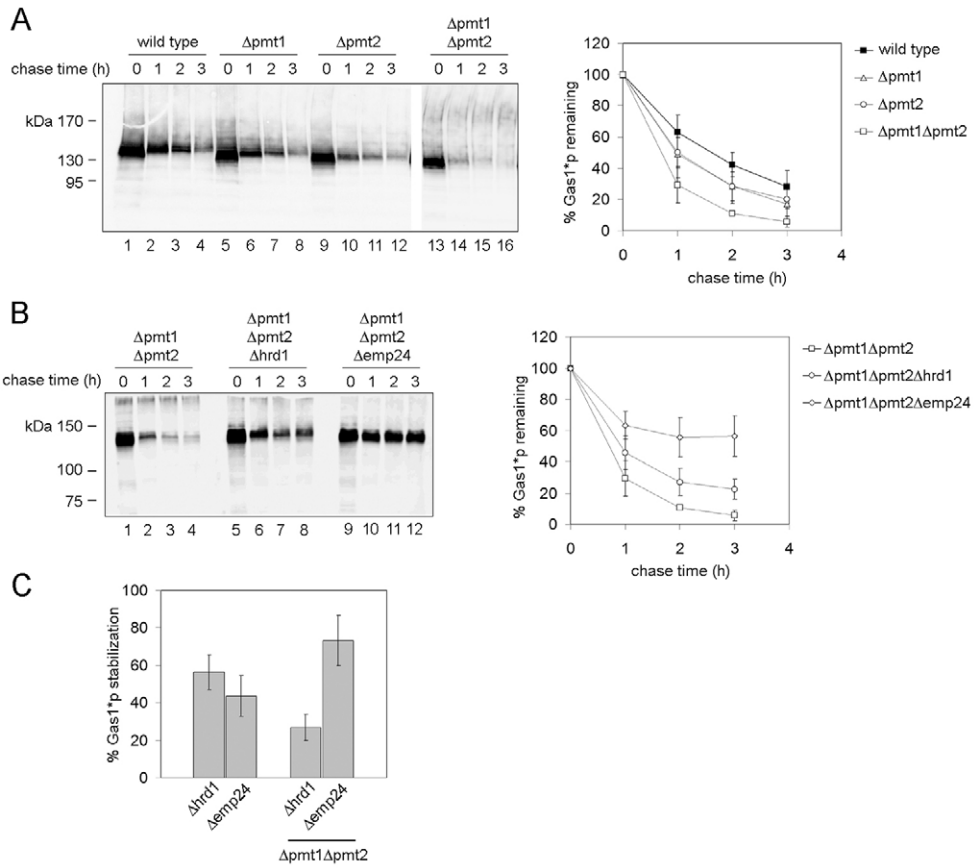

Fig. 4. The Pmt1p–Pmt2p complex has a dual role in the fate of Gas1*p: initial retention of the protein and its ultimate targeting to the Hrd1p complex. (**A**,**B**) Degradation of Gas1*p(HA) in cells carrying the indicated deletions was measured, quantified and plotted as described in Fig. 2. The SDS-PAGE was performed using a 4–20% gradient gel (A) or 5% standard gel (B). (**C**) The degree of Gas1*p(HA) stabilization when depleting the Hrd1p complex was compared with that when depleting the p24 protein complex, both in the absence and presence of the Pmt1p–Pmt2p complex (see Materials and Methods for calculation).

4C). Together with our data for physical interactions (Fig. 1C), these results suggest that the Pmt1p–Pmt2p complex has a dual role in the fate of Gas1*p: first, it retains the protein and prevents its otherwise rapid degradation; and second, it ultimately delivers the protein to the Hrd1p complex-dependent ERAD-L pathway for degradation.

The Pmt1p–Pmt2p complex is required for the fast ER exit of wild-type Gas1p

Because of the association of the Pmt1p–Pmt2p complex with the p24 protein complex, we predicted that the Pmt1p–Pmt2p complex plays a role in ER exit of even wild-type Gas1p. If the Pmt1p–Pmt2p complex possesses a chaperone function, it should promote ER exit of Gas1p. We first tested whether Gas1p would be stable in the absence of the Pmt1p–Pmt2p complex, which would be an indication of its proper folding. To this end, we expressed chromosomally HA-tagged Gas1p in wild-type cells and in Δpmt1Δpmt2 cells and performed a CHX-chase experiment (Fig. 5A, lanes 5–12). As can be seen, Gas1p matured and was stable over a period of several hours in wild-type and in Δpmt1Δpmt2 cells, which was consistent with the wild-type protein being folded properly even in the absence of the Pmt1p–Pmt2p complex. As a control, we show the typical pattern of Gas1*p that is being *O*-mannosylated and degraded in wild-type cells (Fig. 5A, lanes 1–4). We were aware of a minute decrease in electrophoretic mobility of the mature form of Gas1p in Δpmt1Δpmt2 cells compared with wild-type cells, the reason for which is currently unknown (Fig. 5A, compare lanes 5–8 with 9–12). Next, we directly addressed the ER exit kinetics of Gas1p in wild-type cells and in Δpmt1Δpmt2 cells. We performed a radioactive pulse-labeling and chase experiment followed by immunoprecipitation of Gas1p (Fig. 5B). As can be seen, the ER exit of Gas1p was markedly decreased in Δpmt1Δpmt2 cells compared with wild-type cells, as judged by the slower conversion of the precursor form into the mature form. Whereas in wild-type cells about half of the Gas1p was converted into the mature form within 10 minutes, the same process took about 22 minutes in Δpmt1Δpmt2 cells (Fig. 5B). By contrast, the ER exit of endogenous carboxypeptidase Y (CPY) was undisturbed in Δpmt1Δpmt2 cells compared with wild-type cells, showing that the overall kinetics of ER exit were not generally affected (Fig. 5C). These results demonstrate that the Pmt1p–Pmt2p complex promotes ER exit of wild-type Gas1p.

Discussion

We have shown that the Pmt1p–Pmt2p complex possesses previously unknown cellular functions that are reminiscent of those collectively termed ‘ER protein quality control’. The identification of its binding partners and subsequent functional data provide a relatively simple picture and suggest a model for how the Pmt1p–Pmt2p complex performs quality control of ER proteins.

Our data also clarify some puzzling results with regard to the degradation of misfolded GPI-anchored proteins. For instance, although it was reported that Gas1*p is largely degraded by the proteasome, a pathway to the proteasome could not be identified (Fujita et al., 2006). Furthermore, although it was shown that the Pmt1p–Pmt2p complex *O*-mannosylates Gas1*p, it has remained unclear why and where *O*-mannosylated Gas1*p is targeted for degradation (Hirayama et al., 2008).

In the model depicted in Fig. 6, the Pmt1p–Pmt2p complex plays the central and more universal role, whereas the function of

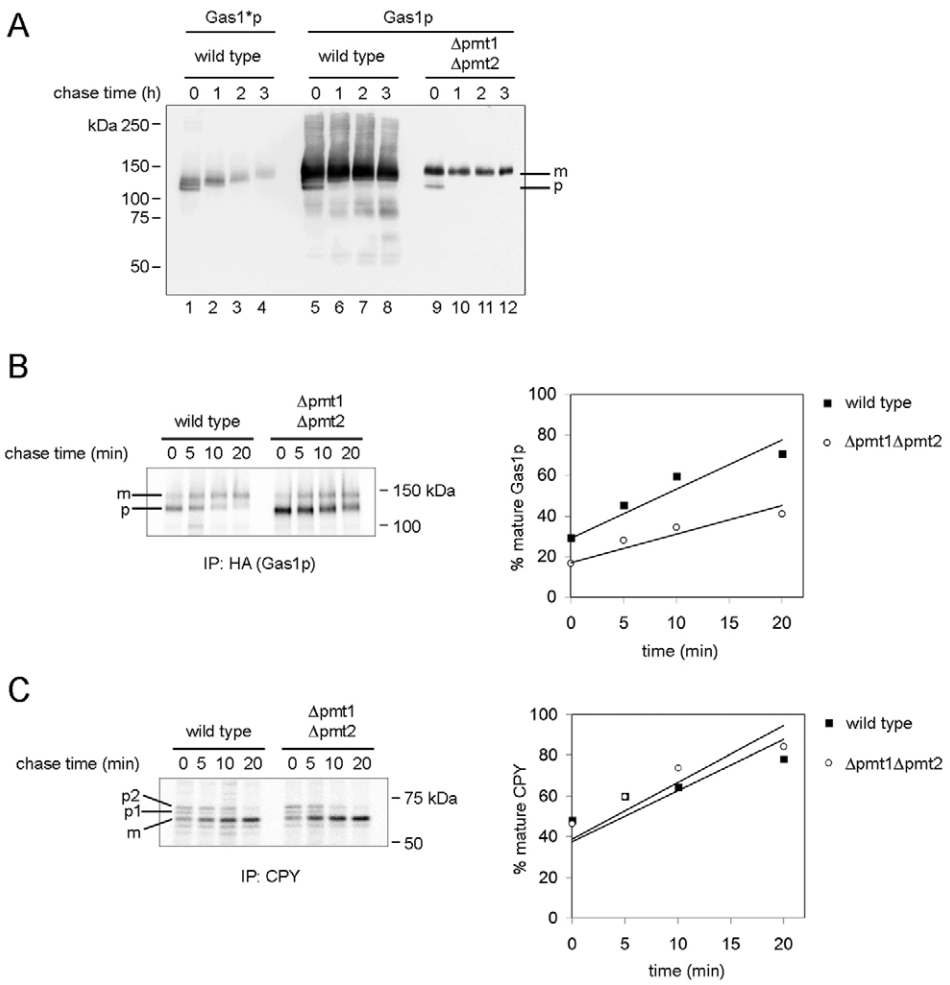

Fig. 5. The Pmt1p–Pmt2p complex promotes ER exit of Gas1p. (**A**) Gas1*p(HA) or Gas1p(HA) were individually expressed in wild-type or in Δpmt1Δpmt2 cells and analyzed as described in Fig. 2. p, precursor form; m, mature form. The SDS-PAGE was performed using a 5% standard gel. (**B**) Yeast cells expressing Gas1p(HA) in wild-type or in Δpmt1Δpmt2 cells were labeled with [35S]methionine for 10 minutes and chased for the indicated times. The cells were lysed and Gas1p(HA) was immunoprecipitated using anti-HA antibodies and analyzed by SDS-PAGE (5% standard gel) and autoradiography. Protein maturation was plotted over time on the basis of the obtained fraction of mature protein form (m) from total protein at indicated times (right panel). Values were obtained using a PhosporImager. The apparent rate for maturation of Gas1p was calculated and shown with linear regression after inclusion of the value zero at time –10 (start of pulse). (**C**) The same experiment with identical cells was performed but the vacuolar peptidase CPY was immunoprecipitated using anti-CPY antibodies. p1, precursor form 1, p2, precursor form 2. Plotting and calculations were done as for B.

the p24 protein complex is restricted to GPI-anchored proteins, like our model proteins Gas1p and Gas1*p. We base the latter assumption on the fact that the p24 protein complex is associated with Gas1p throughout its ER residence time and also during its ER exit (Manuel Muñiz, personal communication). Accordingly, we propose that the Pmt1p–Pmt2p complex binds to Gas1p that is already associated with the p24 protein complex. Because the presence of the Pmt1p–Pmt2p complex promotes fast ER exit of Gas1p (Fig. 5B), the simplest scenario would be that the complex directly or indirectly aids in protein folding (Fig. 6A). This is supported by two observations: first, Ero1p and Pdi1p, which mediate oxidative protein folding, are amongst the binding partners of the Pmt1p–Pmt2p complex (Table 1); and second, mammalian cells express a highly UPR-regulated soluble protein in the ER with homology to the largest luminal loop, loop 5, of the family of PMTs (Fukuda et al., 2001; Hamada et al., 1996). This protein, SDF2L1 in mouse, is also found in complex with other ER resident chaperones (Meunier et al., 2002). Very interestingly, on the basis of the region of homology between SDF2L1, Pmt1p and Pmt2p and on functional studies with Pmt1p (Girrbach et al., 2000), SDF2L1 should be incapable of mediating *O*-mannosylation. This strongly suggests that the proposed chaperone-like function of the Pmt1p–Pmt2p complex is distinct from its *O*-mannosylation activity. Finally, p24 protein complex-dependent ER export of correctly folded Gas1p occurs after dissociation from the Pmt1p–Pmt2p complex, which, in contrast to the p24 protein complex, remains in the ER (Haselbeck and Tanner, 1983; Huh et al., 2003).

Like Gas1p, Gas1*p binds to the p24 protein complex and subsequently to the Pmt1p–Pmt2p complex (Fig. 6B). However, since Gas1*p cannot be folded properly it continuously rebinds to the Pmt1p–Pmt2p complex and is thus retained by it in the ER (Fig. 4 and Fig. 6B). This retention has at least two consequences: first, Gas1*p is increasingly *O*-mannosylated with time in a Pmt1p–Pmt2p complex-dependent manner (Fig. 2, Fig. 5A, Fig. 6B; supplementary material Fig. S1 and Fig. S3); and second, the Pmt1p–Pmt2p complex eventually targets Gas1*p to the Hrd1p complex for ERAD (Fig. 4 and Fig. 6B). The precise molecular role of *O*-mannans in Pmt1p–Pmt2p complex-mediated protein retention and Hrd1p complex-mediated protein degradation is an exciting subject to be addressed next. Because the Pmt1p–Pmt2p complex can associate with the Hrd1p complex protein, *O*-mannosylation should have a function different from targeting proteins to the ERAD machinery. Consistently, *O*-mannosylation is not strictly required for ERAD-dependent degradation of Gas1*p because degradation via the Hrd1p complex still occurs in the absence of the Pmt1p–Pmt2p complex (Fig. 4B). We tested whether the Pmt1p–Pmt2p complex might regulate substrate degradation by *O*-mannosylating ERAD machinery components but found that this is not the case (supplementary material Fig. S4). In another model, increasing *O*-mannosylation of the substrate might help to

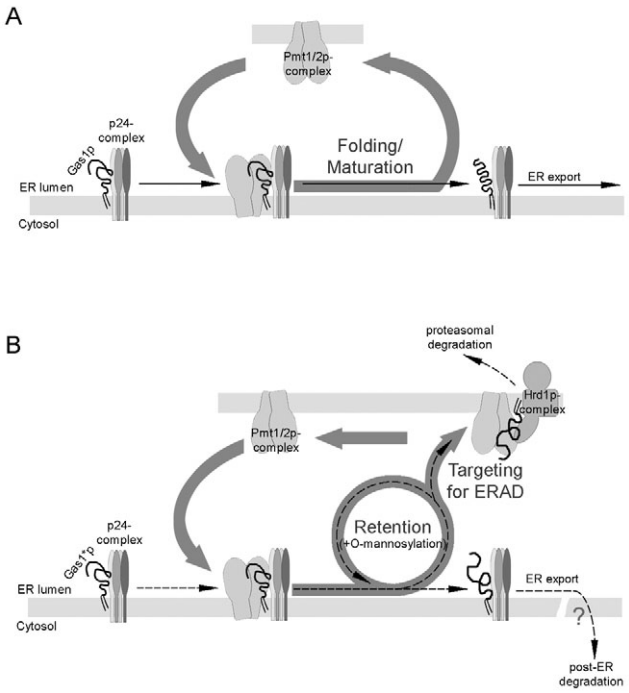

Fig. 6. A model for the role of the Pmt1p–Pmt2p complex in ER protein quality control. The scheme illustrates the proposed role of the Pmt1p–Pmt2p complex in ER protein quality control for the tested model proteins Gas1p and Gas1*p. The basic principle should also be applicable to other substrates (see Discussion). (**A**) ER maturation of Gas1p (solid black arrows). After ER translocation and GPI-anchor transfer and prior to ER export, Gas1p folds and has its GPI anchor remodeled. Gas1p is probably associated to the p24 protein complex throughout its ER residence time. Because the Pmt1p–Pmt2p complex possesses some characteristics of classical chaperones and aids in rapid ER export of Gas1p, it could be involved in protein folding and/or GPI-anchor remodeling (thick gray arrows). (**B**) ER retention and degradation of Gas1*p (dashed black arrows). Like Gas1p, Gas1*p associates with the p24 protein complex. However, an ER export competent fold cannot be achieved, which results in extended association with the Pmt1p–Pmt2p complex ("Retention"), protein *O*-mannosylation ("*O*-mannosylation") and subsequent transfer to the Hrd1p complex ("Targeting for ERAD") for retrotranslocation and proteasomal degradation (see Discussion for details). Those Gas1*p variants that can escape this primary ER quality control (the amount will drastically increase when the Pmt1p–Pmt2p complex is absent) will be subjected to a second, as yet uncharacterized, control system, probably in a post-ER compartment (question mark).

dissociate it from the Pmt1p–Pmt2p complex and allow transfer to the associated ERAD machinery. This model can be tested in the future through the generation and utilization of suitable *O*-mannosylation mutants of the Pmt1p–Pmt2p complex.

Depletion of the Pmt1p–Pmt2p complex leads to an 'escape' of most of the Gas1*p from Hrd1p complex-mediated ERAD to a p24-dependent, probably post-ER, degradation (Figs 4 and 6). Redundant quality control in the ER, although abundant, is probably not too stringent to avoid costly destruction of folding intermediates. However, it becomes clear that the cell possesses additional and less well characterized quality control systems in the secretory pathway downstream of the ER that can target proteins for degradation (Caldwell et al., 2001; Haynes et al., 2002; Vashist et al., 2001; Wang and Ng, 2010). Although we cannot rule out with certainty that the p24 complex is a member of such a post-ER quality control system, we did not find components with known functional links to the proteasome or to the vacuole when we analyzed the binding partners of Emp24p (V.G. and A.M., unpublished data). Thus, the pathway for p24 protein-dependent Gas1*p degradation remains to be identified.

Apart from Gas1*p, the Pmt1p–Pmt2p complex has been shown to *O*-mannosylate several other misfolded soluble or membrane-bound proteins. Examples include KHN, KWW, mutant aspartic protease I and mutant α-factor, none of which are GPI-anchored but all of which are subjected to Hrd1p complex-dependent ERAD (Harty et al., 2001; Nakatsukasa et al., 2004; Vashist et al., 2001; Wahlman et al., 2007). An overall increase in protein *O*-mannosylation has also been observed upon inhibition of *N*-glycosylation, which induces protein misfolding (Harty et al., 2001).

We therefore suggest that the Pmt1p–Pmt2p complex can target a wider variety of misfolded proteins to the Hrd1p complex. One explanation why this conclusion has been missed so far and why there is controversy about the fate of *O*-mannosylated misfolded proteins is that classical tests for involvement of cellular components in protein degradation measure the degree of inhibition of substrate degradation in deletion mutants. However, our data clearly show that the Pmt1p–Pmt2p complex has a retention function on top of its targeting function to the ERAD machinery, which complicates matters. In addition, the cell possesses multiple and apparently very dynamic pathways for protein degradation, which can lead to the targeting of misfolded proteins to different routes upon depletion of one pathway. Considering this, a more combinatorial approach using mutants with disruptions in multiple pathways was needed to obtain better insight into the several functions of the Pmt1p–Pmt2p complex (Fig. 4). The same arguments readily explain the kinetic alterations observed for ER export of Gas1p and for the degradation of Gas1*p in the absence of the Pmt1p–Pmt2p complex. Whereas the export rate of Gas1p was decreased (Fig. 5), the apparent degradation rate of Gas1*p was increased (Fig. 4). With respect to Gas1p, the delay of ER export in the absence of the Pmt1p–Pmt2p complex is consistent with loss of a chaperone that helps rapid folding of Gas1p (Fig. 5B). With respect to Gas1*p, faster degradation by a pathway other than ERAD in the absence of the Pmt1p–Pmt2p complex is consistent with loss of both ER retention and targeting to ERAD (Fig. 4).

Besides its general role in ER protein retention, ERAD and ER export, the Pmt1p–Pmt2p complex might possess an additional and more specific function for the folding and ER export of GPI-anchored proteins. This is suggested by the physical link to the p24 protein complex, as only one of many known ER export factors. Interestingly, we also identified Ted1p as a binding partner of the Pmt1p–Pmt2p complex but not of the p24 protein complex (Table 1; V.G. and A.M., unpublished data). Ted1p was first identified in a screen for proteins impairing the surface expression of mammalian G-protein-activated Kir channel GIRK2 in yeast (Haass et al., 2007). Likewise, the p24 protein complex components Emp24p and Erv25p were among the only six other hits from the 376 tested deletions. It was previously shown that Ted1p and the p24 complex proteins cluster in an epistasis mini-array (E-MAP), which suggested a common biological function (Schuldiner et al., 2005). Indeed, the maturation of Gas1p was delayed in a Ted1p deletion strain similar to an Emp24p deletion strain (Haass et al., 2007). The mammalian ortholog of Ted1p, PAGP5, is a GPI-anchor remodeling enzyme and was recently shown to remove the

side-chain ethanolamine phosphate of the second mannose attached to the GPI-anchor backbone. This activity is prerequisite for efficient ER exit of GPI-anchored proteins (Fujita et al., 2009). In a speculative model, the Pmt1p–Pmt2p complex might regulate access of the Gas1p–p24 protein complex to GPI-anchor remodeling enzymes and thus couple protein folding with GPI-anchor remodeling. This scenario could be part of Pmt1p–Pmt2p complex-mediated Gas1p 'folding', as shown in Fig. 6A.

Materials and Methods

Yeast strains and plasmids

The strains used were isogenic to W303 (*MAT*a *leu2-3,112 trp1-1 can1-100 ura3-1 ade2-1 his3-11,15)* except those used in experiments shown in Fig. 1, Fig. 3A and supplementary material Fig. S2, which were isogenic to BY4741 (*MAT*a *his3*Δ *leu2*Δ *ura3*Δ). Tagging of proteins or genomic gene deletions were performed using standard PCR-based homologous recombination techniques. Gas1*p(HA) was integrated into the URA3 locus of yeast cells using the integrative plasmid pMF616, which was a gift from Morihisa Fujita (Fujita et al., 2006). Gas1p(HA) was derived from pMF616 by back mutation of the single base exchange using standard PCR-based mutagenesis and integrated into the URA3 locus of yeast cells. All constructs were sequenced.

Protein complex purification and co-immunoprecipitation

For mass spectrometry analysis, approximately 15 g of cells were lysed by grinding in liquid nitrogen and the membranes sedimented. Membranes were solubilized in buffer containing 1% digitonin (Calbiochem). The extract was incubated for several hours with IgG-coupled magnetic beads (Dynal). After washing and elution, the eluate was either precipitated with trichloroacetic acid (TCA) or separated by SDS-PAGE, followed by Coomassie Blue staining and excision of individual bands. In both cases, the proteins were identified by mass spectrometry. For co-immunoprecipitation, essentially the same protocol was utilized, with the exception that material from 200 ml cultures were used and cells were lysed using bead beating. After SDS-PAGE, proteins were analyzed by immunblotting with antibodies to HA (Roche) or Usa1p (Carvalho et al., 2006), or with rabbit IgG (Sigma).

Gas1*p(HA) and Gas1p(HA) degradation experiments

Cycloheximide shut-off experiments were performed in exponentially growing cells. The shut-off was started by addition of CHX to a final concentration of 200 µg/ml. Equal volume aliquots of cell culture were removed at indicated time points and moved to ice. Cells were lysed using 150 mM NaOH followed by addition of sample buffer containing 1% SDS and heating. Cellular Gas1*p(HA) or Gas1p(HA) content was probed by SDS-PAGE followed by western blotting using anti-HA antibodies. To quantify bands with the Odyssey Infrared Imaging System (LI-COR Biosciences) a dye-coupled secondary antibody was used (Fig. 2B,C, Fig. 4A; supplementary material Fig. S2). To quantify bands with a LAS-3000 Imaging System (Fujifilm Lifescience) and Multi-Gauge Software, a peroxidase-coupled secondary antibody was used (Fig. 3B, Fig. 4B; supplementary material Fig. S1).

Radioactive pulse-chase and immunoprecipitation

For in vivo pulse labeling, an overnight yeast culture was diluted and grown to an optical density (OD) of ~0.8 at 600 nm. Cells equivalent to 5 OD were resuspended in 1 ml medium lacking methionine, incubated for 15 minutes at 30°C, and labeled for 10 minutes with 100 µCi/ml [^{35}S]methionine (Perkin Elmers). Cells were diluted to OD 0.8, supplemented with methionine and 200 µg/ml CHX. Aliquots were taken at indicated times, cells were moved to ice and supplemented with 10 mM azide, pelleted, resuspended in 50 mM Tris pH 7.5, 5 mM EDTA, 1 mM PMSF, and lysed with glass beads for 7 minutes in a bead-beater, supplemented with 1% SDS, and heated at 65°C for 10 minutes. Cell remnants were removed by centrifugation for 10 minutes in a microfuge, and the supernatant used for immunoprecipitation using anti-HA antibodies. Immune complexes were isolated with Protein G-Sepharose (GE Healthcare) and analyzed by SDS-gel electrophoresis and autoradiography using a PhosphorImager (Fuji).

Calculating Gas1*p stabilization in Δhrd1 and Δemp24 cells in presence or absence of the Pmt1/2p complex as shown in Fig. 4C

Gas1*p turnover in wild-type cells was determined from at least three individual experiments by measuring remaining Gas1*p by western blotting as shown in Fig. 2B. The obtained values for individual timepoints were used for linear regression using the least square method (LINEST function in EXCEL). We obtained R^2 values of 0.9344 or higher for each data set. The m values ($y=mx+b$) for each individual regression set were calculated, as well as the mean value and its standard deviation. We then compared the m value obtained with wild-type cells with those obtained with single deletion mutants (Δemp24 and Δhrd1). The deviation in m values of mutants from those obtained with wild-type cells was taken as degree of stabilization (stab=m_{mut}/m_{wt}). Because we found Gas1*p is maximally stable in Δemp24Δhrd1 cells compared to the individual mutants (Fig. 3B), we assumed separate degradation pathways and combined the individual determined degrees of stabilization to 100% ($stab_{\Delta emp24}+stab_{\Delta hrd1}=100$). Lastly, we plotted the degree of Gas1*p stabilization for each mutant as a percentage of total, either in the presence of the Pmt1p–Pmt2p complex (Δhrd1 vs Δemp24) or in its absence (Δhrd1Δpmt1Δpmt2 vs Δemp24Δpmt1Δpmt2).

We would like to thank Pedro Carvalho (CRG, Barcelona, Spain) and Manuel Muñiz (University of Seville, Seville, Spain) for antibodies, Morihisa Fujita (Osaka University, Osaka, Japan) for plasmids and Ross Tomaino (Harvard Medical School, Boston, MA) for excellent mass spectrometric analysis, Alex Palazzo, Tom Rapoport, Martin Spiess and Karl Erlandson for critical reading of an earlier version of the manuscript; and Manuel Muñiz and Leticia Lemus for very fruitful discussions throughout the work. V.G. is supported by a Grant of the Spanish Ministry of Science, BFU2009-07290. V.G. is a Ramon y Cajal fellow.

Supplementary material available online at
http://jcs.biologists.org/cgi/content/full/124/1/144/DC1

References

Ballif, B. A., Roux, P. P., Gerber, S. A., MacKeigan, J. P., Blenis, J. and Gygi, S. P. (2005). Quantitative phosphorylation profiling of the ERK/p90 ribosomal S6 kinase-signaling cassette and its targets, the tuberous sclerosis tumor suppressors. *Proc. Natl. Acad. Sci. USA* **102**, 667-672.

Barlowe, C. (2003). Signals for COPII-dependent export from the ER: what's the ticket out? *Trends Cell. Biol.* **13**, 295-300.

Brachmann, C. B., Davies, A., Cost, G. J., Caputo, E., Li, J., Hieter, P. and Boeke, J. D. (1998). Designer deletion strains derived from Saccharomyces cerevisiae S288C: a useful set of strains and plasmids for PCR-mediated gene disruption and other applications. *Yeast* **14**, 115-132.

Brodsky, J. L., Werner, E. D., Dubas, M. E., Goeckeler, J. L., Kruse, K. B. and McCracken, A. A. (1999). The requirement for molecular chaperones during endoplasmic reticulum-associated protein degradation demonstrates that protein export and import are mechanistically distinct. *J. Biol. Chem.* **274**, 3453-3460.

Caldwell, S. R., Hill, K. J. and Cooper, A. A. (2001). Degradation of endoplasmic reticulum (ER) quality control substrates requires transport between the ER and Golgi. *J. Biol. Chem.* **276**, 23296-23303.

Carvalho, P., Goder, V. and Rapoport, T. A. (2006). Distinct ubiquitin-ligase complexes define convergent pathways for the degradation of ER proteins. *Cell* **126**, 361-373.

Denic, V., Quan, E. M. and Weissman, J. S. (2006). A luminal surveillance complex that selects misfolded glycoproteins for ER-associated degradation. *Cell* **126**, 349-359.

Dieguez-Acuna, F. J., Gerber, S. A., Kodama, S., Elias, J. E., Beausoleil, S. A., Faustman, D. and Gygi, S. P. (2005). Characterization of mouse spleen cells by subtractive proteomics. *Mol. Cell Proteomics* **4**, 1459-1470.

Ellgaard, L. and Helenius, A. (2003). Quality control in the endoplasmic reticulum. *Nat. Rev. Mol. Cell Biol.* **4**, 181-191.

Fra, A. M., Fagioli, C., Finazzi, D., Sitia, R. and Alberini, C. M. (1993). Quality control of ER synthesized proteins: an exposed thiol group as a three-way switch mediating assembly, retention and degradation. *EMBO J.* **12**, 4755-4761.

Fujita, M., Yoko, O. T. and Jigami, Y. (2006). Inositol deacylation by Bst1p is required for the quality control of glycosylphosphatidylinositol-anchored proteins. *Mol. Biol. Cell* **17**, 834-850.

Fujita, M., Maeda, Y., Ra, M., Yamaguchi, Y., Taguchi, R. and Kinoshita, T. (2009). GPI glycan remodeling by PGAP5 regulates transport of GPI-anchored proteins from the ER to the Golgi. *Cell* **139**, 352-365.

Fukuda, S., Sumii, M., Masuda, Y., Takahashi, M., Koike, N., Teishima, J., Yasumoto, H., Itamoto, T., Asahara, T., Dohi, K. et al. (2001). Murine and human SDF2L1 is an endoplasmic reticulum stress-inducible gene and encodes a new member of the Pmt/rt protein family. *Biochem. Biophys. Res. Commun.* **280**, 407-414.

Girrbach, V. and Strahl, S. (2003). Members of the evolutionarily conserved PMT family of protein O-mannosyltransferases form distinct protein complexes among themselves. *J. Biol. Chem.* **278**, 12554-12562.

Girrbach, V., Zeller, T., Priesmeier, M. and Strahl-Bolsinger, S. (2000). Structure-function analysis of the dolichyl phosphate-mannose: protein O-mannosyltransferase ScPmt1p. *J. Biol. Chem.* **275**, 19288-19296.

Goder, V., Carvalho, P. and Rapoport, T. A. (2008). The ER-associated degradation component Der1p and its homolog Dfm1p are contained in complexes with distinct cofactors of the ATPase Cdc48p. *FEBS Lett* **582**, 1575-1580.

Haass, F. A., Jonikas, M., Walter, P., Weissman, J. S., Jan, Y. N., Jan, L. Y. and Schuldiner, M. (2007). Identification of yeast proteins necessary for cell-surface function of a potassium channel. *Proc. Natl. Acad. Sci. USA* **104**, 18079-18084.

Hamada, T., Tashiro, K., Tada, H., Inazawa, J., Shirozu, M., Shibahara, K., Nakamura, T., Martina, N., Nakano, T. and Honjo, T. (1996). Isolation and characterization of a novel secretory protein, stromal cell-derived factor-2 (SDF-2) using the signal sequence trap method. *Gene* **176**, 211-214.

Hammond, C., Braakman, I. and Helenius, A. (1994). Role of N-linked oligosaccharide recognition, glucose trimming, and calnexin in glycoprotein folding and quality control. *Proc. Natl. Acad. Sci. USA* **91**, 913-917.

Harty, C., Strahl, S. and Romisch, K. (2001). O-mannosylation protects mutant alpha-factor precursor from endoplasmic reticulum-associated degradation. *Mol. Biol. Cell* **12**, 1093-1101.

Haselbeck, A. and Tanner, W. (1983). O-glycosylation in Saccharomyces cerevisiae is initiated at the endoplasmic reticulum. *FEBS Lett.* **158**, 335-338.

Haynes, C. M., Caldwell, S. and Cooper, A. A. (2002). An HRD/DER-independent ER quality control mechanism involves Rsp5p-dependent ubiquitination and ER-Golgi transport. *J. Cell Biol.* **158**, 91-101.

Hellman, R., Vanhove, M., Lejeune, A., Stevens, F. J. and Hendershot, L. M. (1999). The in vivo association of BiP with newly synthesized proteins is dependent on the rate and stability of folding and not simply on the presence of sequences that can bind to BiP. *J. Cell Biol.* **144**, 21-30.

Hettema, E. H., Valdez-Taubas, J. and Pelham, H. R. (2004). Bsd2 binds the ubiquitin ligase Rsp5 and mediates the ubiquitination of transmembrane proteins. *EMBO J.* **23**, 1279-1288.

Hirayama, H., Fujita, M., Yoko-o, T. and Jigami, Y. (2008). O-mannosylation is required for degradation of the endoplasmic reticulum-associated degradation substrate Gas1*p via the ubiquitin/proteasome pathway in Saccharomyces cerevisiae. *J. Biochem.* **143**, 555-567.

Hong, E., Davidson, A. R. and Kaiser, C. A. (1996). A pathway for targeting soluble misfolded proteins to the yeast vacuole. *J. Cell Biol.* **135**, 623-633.

Huh, W. K., Falvo, J. V., Gerke, L. C., Carroll, A. S., Howson, R. W., Weissman, J. S. and O'Shea, E. K. (2003). Global analysis of protein localization in budding yeast. *Nature* **425**, 686-691.

Kincaid, M. M. and Cooper, A. A. (2007). Misfolded proteins traffic from the endoplasmic reticulum (ER) due to ER export signals. *Mol. Biol. Cell* **18**, 455-463.

Lussier, M., Gentzsch, M., Sdicu, A. M., Bussey, H. and Tanner, W. (1995). Protein O-glycosylation in yeast. The PMT2 gene specifies a second protein O-mannosyltransferase that functions in addition to the PMT1-encoded activity. *J. Biol. Chem.* **270**, 2770-2775.

McCracken, A. A. and Brodsky, J. L. (1996). Assembly of ER-associated protein degradation in vitro: dependence on cytosol, calnexin, and ATP. *J. Cell Biol.* **132**, 291-298.

Meunier, L., Usherwood, Y. K., Chung, K. T. and Hendershot, L. M. (2002). A subset of chaperones and folding enzymes form multiprotein complexes in endoplasmic reticulum to bind nascent proteins. *Mol. Biol. Cell* **13**, 4456-4469.

Meusser, B., Hirsch, C., Jarosch, E. and Sommer, T. (2005). ERAD: the long road to destruction. *Nat. Cell Biol.* **7**, 766-772.

Muniz, M., Nuoffer, C., Hauri, H. P. and Riezman, H. (2000). The Emp24 complex recruits a specific cargo molecule into endoplasmic reticulum-derived vesicles. *J. Cell Biol.* **148**, 925-930.

Muniz, M., Morsomme, P. and Riezman, H. (2001). Protein sorting upon exit from the endoplasmic reticulum. *Cell* **104**, 313-320.

Nakatsukasa, K., Okada, S., Umebayashi, K., Fukuda, R., Nishikawa, S. and Endo, T. (2004). Roles of O-mannosylation of aberrant proteins in reduction of the load for endoplasmic reticulum chaperones in yeast. *J. Biol. Chem.* **279**, 49762-49772.

Parodi, A. J. (2000). Protein glucosylation and its role in protein folding. *Annu. Rev. Biochem.* **69**, 69-93.

Plemper, R. K., Bohmler, S., Bordallo, J., Sommer, T. and Wolf, D. H. (1997). Mutant analysis links the translocon and BiP to retrograde protein transport for ER degradation. *Nature* **388**, 891-895.

Rabinovich, E., Kerem, A., Frohlich, K. U., Diamant, N. and Bar-Nun, S. (2002). AAA-ATPase p97/Cdc48p, a cytosolic chaperone required for endoplasmic reticulum-associated protein degradation. *Mol. Cell Biol.* **22**, 626-634.

Reggiori, F. and Pelham, H. R. (2002). A transmembrane ubiquitin ligase required to sort membrane proteins into multivesicular bodies. *Nat. Cell Biol.* **4**, 117-123.

Schimmoller, F., Singer-Kruger, B., Schroder, S., Kruger, U., Barlowe, C. and Riezman, H. (1995). The absence of Emp24p, a component of ER-derived COPII-coated vesicles, causes a defect in transport of selected proteins to the Golgi. *EMBO J.* **14**, 1329-1339.

Schuldiner, M., Collins, S. R., Thompson, N. J., Denic, V., Bhamidipati, A., Punna, T., Ihmels, J., Andrews, B., Boone, C., Greenblatt, J. F. et al. (2005). Exploration of the function and organization of the yeast early secretory pathway through an epistatic miniarray profile. *Cell* **123**, 507-519.

Spiro, R. G. (2002). Protein glycosylation: nature, distribution, enzymatic formation, and disease implications of glycopeptide bonds. *Glycobiology* **12**, 43R-56R.

Strahl-Bolsinger, S. and Scheinost, A. (1999). Transmembrane topology of pmt1p, a member of an evolutionarily conserved family of protein O-mannosyltransferases. *J. Biol. Chem.* **274**, 9068-9075.

Strahl-Bolsinger, S., Immervoll, T., Deutzmann, R. and Tanner, W. (1993). PMT1, the gene for a key enzyme of protein O-glycosylation in Saccharomyces cerevisiae. *Proc. Natl. Acad. Sci. USA* **90**, 8164-8168.

Swanson, R., Locher, M. and Hochstrasser, M. (2001). A conserved ubiquitin ligase of the nuclear envelope/endoplasmic reticulum that functions in both ER-associated and Matalpha2 repressor degradation. *Genes Dev.* **15**, 2660-2674.

Travers, K. J., Patil, C. K., Wodicka, L., Lockhart, D. J., Weissman, J. S. and Walter, P. (2000). Functional and genomic analyses reveal an essential coordination between the unfolded protein response and ER-associated degradation. *Cell* **101**, 249-258.

Vashist, S., Kim, W., Belden, W. J., Spear, E. D., Barlowe, C. and Ng, D. T. (2001). Distinct retrieval and retention mechanisms are required for the quality control of endoplasmic reticulum protein folding. *J. Cell Biol.* **155**, 355-368.

Wahlman, J., DeMartino, G. N., Skach, W. R., Bulleid, N. J., Brodsky, J. L. and Johnson, A. E. (2007). Real-time fluorescence detection of ERAD substrate retrotranslocation in a mammalian in vitro system. *Cell* **129**, 943-955.

Wang, S. and Ng, D. T. (2010). Evasion of endoplasmic reticulum surveillance makes Wsc1p an obligate substrate of Golgi quality control. *Mol. Biol. Cell* **21**, 1153-1165.

Willer, T., Valero, M. C., Tanner, W., Cruces, J. and Strahl, S. (2003). O-mannosyl glycans: from yeast to novel associations with human disease. *Curr. Opin. Struct. Biol.* **13**, 621-630.

Ye, Y., Meyer, H. H. and Rapoport, T. A. (2001). The AAA ATPase Cdc48/p97 and its partners transport proteins from the ER into the cytosol. *Nature* **414**, 652-656.

Zhang, J. X., Braakman, I., Matlack, K. E. and Helenius, A. (1997). Quality control in the secretory pathway: the role of calreticulin, calnexin and BiP in the retention of glycoproteins with C-terminal truncations. *Mol. Biol. Cell* **8**, 1943-1954.

Journal of Cell Science